Slk19p Is a Centromere Protein That Functions to Stabilize Mitotic Spindles

Xuemei Zeng,* Jason A. Kahana,‡ Pamela A. Silver,‡ Mary K. Morphew,§ J. Richard McIntosh,§ Ian T. Fitch,‖ John Carbon,‖ and William S. Saunders*

*Department of Biological Sciences, University of Pittsburgh, Pittsburgh, Pennsylvania 15260; ‡Department of Biological Chemistry and Molecular Pharmacology, Harvard Medical School and The Dana Farber Cancer Institute, Boston, Massachusetts 02115; §Department of Molecular, Cell, and Developmental Biology, University of Colorado, Boulder, Colorado 80309-0347; and ‖Department of Molecular, Cellular, and Developmental Biology, University of California, Santa Barbara, California 93106

Abstract. We have identified a novel centromere-associated gene product from *Saccharomyces cerevisiae* that plays a role in spindle assembly and stability. Strains with a deletion of *SLK19* (*synthetic lethal Kar3p* gene) exhibit abnormally short mitotic spindles, increased numbers of astral microtubules, and require the presence of the kinesin motor Kar3p for viability. When cells are deprived of both Slk19p and Kar3p, rapid spindle breakdown and mitotic arrest is observed. A functional fusion of Slk19p to green fluorescent protein (GFP) localizes to kinetochores and, during anaphase, to the spindle midzone, whereas Kar3p-GFP was found at the nuclear side of the spindle pole body. Thus, these proteins seem to play overlapping roles in stabilizing spindle structure while acting from opposite ends of the microtubules.

Key words: spindle • *Saccharomyces cerevisiae* • kinetochore • motor • yeast

During division, the eucaryotic cell must assemble a complex array of interphase microtubules (Mts)[1] and chromosomes into a bipolar spindle. For this structure to be functional, the dynamic nature of the Mts must be controlled, so that they persist long enough for a stable association between the chromosomes and the centrosome to form. Mts in dividing cells are mostly anchored at the centrosome, but have free and dynamic plus ends that can grow and shrink rapidly while they search for chromosome attachments (Holy and Leibler, 1996).

Once the Mt associates with the kinetochore complex of a chromosome, the dynamic instability of the plus ends is suppressed. This increased stability of kinetochore microtubules (k-Mts) has been documented in numerous studies. k-Mts are more resistant than nonkinetochore polar Mts to the depolymerizing drug colchicine (Salmon et al., 1984), cold (Brinkley and Cartwright, 1975; Rieder, 1981), calcium (Salmon and Segall, 1980), and change in hydrostatic pressure (Salmon et al., 1976). Photoactivation of caged fluorescein-labeled tubulin has indicated that polar Mts turn over with a half life of ~1 min, whereas k-Mts turn over with a half life of ~4.7 min (Zhai et al., 1995). Treatment of PtK_1 cells with nocodazole shows that k-Mts persist about ten times longer than polar Mts (Cassimeris et al., 1990). k-Mts are not completely blocked at their plus ends because tubulin subunits can be incorporated or lost at the kinetochores while the chromosomes remain attached (Mitchison et al., 1986), but these studies clearly show the enhanced stability of k-Mts compared with polar Mts.

Two lines of evidence indicate that the increased stability of k-Mts probably is due to factors that are associated with the kinetochore itself. First, when Mts are forcibly detached from kinetochores, they quickly depolymerize (Nicklas and Kubai, 1985). Secondly, association with kinetochores can stabilize preformed Mts in vitro (Mitchison and Kirschner, 1985). While kinetochores are known to promote Mt stability, the proteins involved have not yet been identified.

There is a growing body of evidence that Mt stability

Xuemei Zeng and Jason A. Kahana contributed equally to the manuscript.

Jason A. Kahana's current address is Ludwig Institute for Cancer Research, University of California, San Diego, CA 92093-0660.

Address correspondence to W. Saunders, Department of Biological Sciences, 258 Crawford Hall, University of Pittsburgh, Pittsburgh, PA 15260. Tel.: (412) 624-4320. Fax: (412) 624-4759. E-mail: wsaund+@pitt.edu

1. *Abbreviations used in this paper:* 5-FOA, 5-fluororotic acid; ChIP, chromatin immunoprecipitation assay; DAPI, 4′,6-diamidino-2-phenylindole; GFP, green fluorescent protein; HU, hydroxyurea; k-Mts, kinetochore microtubules; Mts, microtubules; ORF, open reading frame; *SLK19*, *synthetic lethal Kar3p* gene; SPB, spindle pole body; ts, temperature sensitive.

can be directly influenced by Mt-based molecular motors. The first example of this was the yeast motor Kar3p. Kar3p is a minus end directed kinesin-related protein that destabilizes Mts in vitro, preferentially at their minus ends (Endow et al., 1994). In vivo, Kar3p is located predominantly at the spindle poles, typically the position of the minus ends of the Mts (Page et al., 1993; Saunders et al., 1997a; Manning, 1999). *kar3* mutants show an increase in the length and number of cytoplasmic Mts (Saunders et al., 1997a), and grow better under conditions that destabilize Mts (Roof et al., 1991; Saunders et al., 1997a). A spindle collapse that is observed upon the loss of the pole separating motors Cin8p and Kip1p is thought to be mediated by Kar3p (Saunders and Hoyt, 1992), and is markedly delayed by a tubulin mutant that produces hyperstable Mts (Saunders et al., 1997b). These observations indicate that Kar3p is required for some aspect of normal Mt polymerization or dynamics in the cell. The most detailed demonstration of motor control of Mt dynamics is from the in vitro analysis of XKCM1. Recent work has shown that this protein can bind to and stimulate Mt depolymerization from either the plus or minus ends of the Mt. The protein apparently uses the ATPase activity not for translocation, but to recycle off the tubulin subunit and rebind a new Mt end (Desai et al., 1999).

To identify proteins modifying Mt dynamics and spindle structure further, we searched for novel genes that are required for cell viability when Kar3p is absent. One such gene, *SLK19* (*synthetic lethal Kar3p*, previously *SMS1*), was identified. *SLK19* does not encode a conserved motor domain, but when deleted, a mitotic phenotype similar to loss of *KAR3* is observed. *slk19* mutants are viable, but exhibit decreased spindle length and increased numbers of cytoplasmic Mts. When both the *SLK19* and *KAR3* gene products are missing or defective, cells arrest in mitosis and are unable to assemble a spindle. If spindles are assembled first and the cells are then deprived of Slk19p and Kar3p, the nuclear spindle disassembles and collapses, and the cytoplasmic Mts grow in number and length. A functional fusion of Slk19p to green fluorescent protein (GFP) localizes to kinetochores and the spindle midzone during mitosis. Taken together, these findings suggest that Slk19p functions as a spindle Mt-stabilizing protein by associating with the plus ends of Mts at the kinetochore and in the vicinity of the spindle midzone.

Materials and Methods

Yeast Strains, Plasmids, and Media

The strains used in these experiments are derivatives of S288C and are shown in Table I. Media have been described in Sherman et al. (1983). Hydroxyurea (HU) arrest was applied to log phase cultures at 0.1 M HU, pH 5.8, at 30°C for 3.5 h. The arrest was confirmed by examining cells fixed in 70% ethanol after staining with the DNA-specific fluorescent dye 4′,6-diamidino-2-phenylindole (DAPI; Sigma Chemical Co.) at 1 μg/ml.

kar3Δ Synthetic Lethal Mutational Screen

A *kar3*Δ strain, WSY69, was transformed with a *KAR3-URA3* plasmid (pMR798) and mutagenized with ethyl methyl sulphonate (EMS), as described by Kassir and Simchen (1991), to ~30% survival. The treated cells were grown on yeast extract peptone dextrose (YEPD) plates at ~400 colonies per plate and then replica plated to 5-fluororotic acid (5-FOA) plates. Approximately 9,000 mutagenized *kar3*Δ p*KAR3-URA3* cells were screened and 20 mutants were selected that failed to survive on 5-FOA. One mutant, while FOA sensitive, failed to grow on plates lacking uracil, suggesting it no longer contained the original *KAR3-URA3* plasmid and was discarded. For 11 mutants, 5-FOA sensitivity segregated as a single gene mutation, and growth on 5-FOA was possible if *KAR3* was provided on a *HIS3* vector. These mutants were tested by mutual crossings and fell into eight complementation groups, one of which is represented by *SLK19*.

Table I. Genotypes and Plasmids Used in this Study

Yeast strains	Relevant genotype	Yeast strains	Relevant genotype
JKY292	*kar3::KAR3-GFP:URA3*	JKY288	*slk19::SLK19:GFP:URA3*
JKY288	*cbf2::CBF2-GFP:URA3*	WSY68	*kar3::LEU2*
WSY69	*kar3::LEU2*	WSY218	*kar3::LEU2* pMR798
WSY283	*cin8-3*	WSY546	*kar3::LEU2*
WSY684	*kip3::HIS3*	WSY601	*cin8::LEU2* pMA1125
WSY782	*kar3::LEU2 slk19::HIS3* pMR798	WSY813	*slk19::HIS3*
WSY942	*cin8::LEU2 slk19::HIS3* pMA1125	WSY985	*kip2::URA3 slk19::HIS3 kar3::LEU2* pXZB42
WSY987	*kar3::LEU2 slk19::HIS3* pXZB42	WSY990	*slk19::SLK19-GFP:URA3*
WSY991	*dyn1::HIS3 kar3::LEU2* pXZB42	WSY998	*slk19::SLK19-GFP:URA3*
WSY1005	*slk19::HIS3 cin8-3*	316B	*cbf2Δ::TRP1* p*CEN URA3 CBF2*

Plasmids	Relevant plasmid loci
pMR798	*KAR3-URA3-CEN*
pMA1125	*CIN8-URA3-CEN*
pXZB2	*KAR3-HIS3-CEN*
pXZB17	*SLK19* in pUC18-*URA3*
pJK143	*TRP1 SLK19-GFP CEN*
pJK145	*SLK19-GFP-NUF2 3′ UTR URA3* integrating vector
pJK171	*CBF2-GFP-NUF2 3′ UTR URA3* integrating vector
pJK152	*KAR3-GFP-NUF2 3′ UTR URA3* integrating vector
pXZB18	*slk19::HIS3* in pUC18-*URA3*
pXZB42	*kar3-ts* in pRS200 (*TRP1-CEN*)
pXZB10	*SLK19 HIS3 CEN*

Double colon refers to a deletion of the preceding gene and replacement by the marker gene that follows. A single colon refers to linkage without disruption.

Cloning of SLK19

The EMS-generated *slk19-1* mutant is recessive and was backcrossed twice to a *kar3*Δ mutant (WSY68). The 5-FOA sensitivity segregated 2:2 in a total of 14 tetrads demonstrating a single mutant locus. The *SLK19* gene was cloned by complementation with a *TRP1-CEN* plasmid library (created by F. Spencer and P. Hieter; Johns Hopkins Medical School, Baltimore, MD) by selection for growth on 5-FOA. Restriction enzyme analysis revealed two populations of suppressing plasmids, one of which contained *KAR3*, an expected positive. One representative of the second plasmid group was sequenced at the ends of the insert and the genome position identified by a search of the Stanford *Saccharomyces* Genomic Database. Deletion analysis showed that only YOR195w rescued the *slk19*Δ *kar3*Δ lethality. The gene identity was confirmed with the disruption allele.

Disruption of SLK19

To generate a YOR195w deletion strain, a BglII/XhoI fragment containing 67% of the YOR195w coding sequence, from amino acid 58 to 607, on pXZB17 was replaced by a BamHI/XhoI fragment containing *HIS3* gene from pUC18-*HIS3*. A linearized DNA fragment from the resulting plasmid (pXZB18) containing the disrupted YOR195w was transformed into a *kar3*Δ pMR798 (*URA3-KAR3*; Meluh and Rose, 1990) strain to replace the wild-type YOR195w. his^+ transformants were replica plated onto 5-FOA plates to select for transformants that were unable to grow on 5-FOA.

To confirm that *YOR195w::HIS3* is a disruption of the *slk19-1* locus, a *YOR195w::HIS3 kar3*Δ double mutant was crossed to a *slk19-1 kar3*Δ strain. No 5-FOA resistant recombinants were observed for seven tetrads, indicating lack of recombination between the *slk19-1* and *YOR195w::HIS3* loci. The *YOR195w::HIS3* mutation also has the Mt array defects of the *slk19-1* mutation, *slk19-1*/*YOR195w::HIS3 kar3*Δ/*kar3*Δ diploids with pMR798 could not grow on 5-FOA, and the *YOR195w::HIS3 kar3*Δ p*kar3-ts* (temperature sensitive) double mutant had the mitotic arrest phenotype of the *slk19-1 kar3*Δ p*kar3-ts* strain. We interpret these results to indicate that YOR195w is the wild-type allele of the *slk19-1* mutant locus. All analysis of the *slk19* mutant phenotype in this manuscript was with the *YOR195w::HIS3* deletion allele (*slk19*Δ).

Construction of a KAR3 Temperature Sensitive Allele

A *KAR3 ts* allele was generated by random PCR mutagenesis. Two primers were designed that correspond to the COOH-terminal half of *KAR3*: GDp 11 (forward primer), TTA CGA CGC GTA TGA AGC TAT C (MluI is underlined); and GDp 14 (reverse primer), GAA GGC CTT GAC CTC ATT TT (StuI is underlined). pXZB2, with the wild-type allele of *KAR3*, was used as the template for the PCR reaction using Taq polymerase under the following conditions: 1.0 μM GDp11, 1.0 μM GDp14, 50 μM dATP, 100 μM dCTP, 100 μM dGTP, 100 μM dTTP, 1 mM $MgCl_2$, and 0.02 ng/μl template.

The PCR product was digested by MluI and StuI, and was used to replace the MluI/StuI fragment in pXZB2. Plasmids were transformed into a *kar3*Δ strain to identify an allele that supported karyogamy at 26°C, but not 35°C. Two candidates were identified and transformed into all eight *kar3*Δ synthetic lethal mutants identified in our genetic screen. Only one allele allowed the *kar3* synthetic lethal mutant cells to survive without *KAR3-URA3* plasmid at 26°C, but not at 35°C.

Immunofluorescence Microscopy

Antitubulin indirect immunofluorescence was performed on formaldehyde-fixed cells using mAb YOL 1/34 (Serotec Ltd.), rhodamine-conjugated secondary antibody (Jackson ImmunoResearch Laboratories, Inc.), and DAPI to identify the position of the nucleus as described (Pringle et al., 1991; Hoyt et al., 1992). The slides were examined with an Olympus BX60 epifluorescence microscope using a 100× oil immersion objective. Digital images were captured with a Hamamatsu Argus-20 CCD camera and image processor. To increase the percentage of cells in the correct focal plane, photo images of antitubulin staining (see Figs. 1 A and 5 A) are montages made by combining relevant portions of selected captured images taken from a single sample using the Adobe Photoshop software. Mt arrays were chosen based on clarity and uniform plane of focus throughout the spindle, and care was taken to pick a representative sample. Images were processed with the Photoshop program to create a uniform background. Spindle pole and tubulin double-labeling followed the same general procedure as antitubulin indirect immunofluorescence. The antibodies were added in the following order: mouse anti-90 kD (without dilution, a gift of J. Kilmartin), rhodamine-conjugated anti-mouse antibody (1:1,000 dilution; Sigma Chemical Co.), YOL1/34, and fluorescence-conjugated anti-rat antibody (1:100 dilution; Jackson ImmunoResearch Laboratories, Inc.).

Mt length measurements were made from captured antitubulin fluorescent images using the Argus-20 image processor cursor-based measuring capability. Calibration of the measurement software program was performed by use of an engraved slide (Olympus Optical Co.). The chromosome spread procedure was as described (Loidl et al., 1998), except that cells were treated with 10 μg/ml Zymolyase-20T instead of Zymolyase-100T for 2 h.

EM Immunocytochemistry

Immunoelectron microscopy localization of Slk19p was as described in Ding et al. (1997). Cells were harvested from a log phase culture by vacuum filtration, fast-frozen with liquid nitrogen in a Balzers HPM10 high pressure freezer, and then freeze-substituted in 0.1% anhydrous glutaraldehyde dissolved in acetone at −90°C. GFP was localized with an affinity-purified polyclonal rabbit antibody (raised by J. Kahana and P. Silver) diluted to ~10 mg/ml with a blocking buffer containing PBS, 0.02% Tween-80, 0.8% BSA, and 0.1% fish gelatin (Nycomed Amersham Inc.). Sections mounted on grids were floated overnight on a 20 ml drop of this solution at 4°C in a small chamber saturated with water vapor. The grids were then rinsed in PBS containing 0.1% Tween-80 and stained for 2 h at room temperature with goat anti–rabbit immunoglobulin labeled with 10–nm colloidal gold (British Biocell) diluted 1:20 with blocking buffer. The grids were then fixed in 0.5% glutaraldehyde in PBS, stained with uranyl acetate and lead citrate, dried, and examined in a Philips CM10 electron microscope operating at 80 kV.

Chromatin Immunoprecipitation

In vivo cross-linking and chromatin immunoprecipitation were performed essentially as described by Meluh and Koshland (1997). Cross-linked chromatin corresponding to 15 OD_{600} units of cells was immunoprecipitated with affinity-purified anti-GFP or anti-Cbf2p antibodies at a final concentration of 5 mg/ml. Total input DNA was isolated from cross-linked chromatin corresponding to 3 OD_{600} units of cells. Total DNA (1/40 total yield) and coimmunoprecipitated DNA (1/8 total yield) was analyzed by PCR (24 cycles) using pairs of primers corresponding to the following loci: *CEN3*, 5′-ATCAGCGCCAAACAATATGG-3′ and 5′-GAGCAAAACTTCCACCAGT A-3′; *CEN16*, 5′-TTGAAGCCGTTATGTTGTCG-3′ and 5′-TACCATGGTGTGTCAC TTCC-3′; *ARS2*, 5′-GACCGCCATTTCGAACGGAA-3′ and 5′-CGTGAGTACTAAT AAACGGA-3′; and *MET2*, 5′-AGATCCCAACTACTTGGACG-3′ and 5′-GGACACCACGCTTTGACCTT-3′. PCR products (1/5 reaction for total DNA, 2/5 reaction for coimmunoprecipitated DNA) were run on 2% agarose gels and visualized with ethidium bromide.

GFP Fusions

SLK19–GFP Fusion Plasmids. pJK143 is a *CEN TRP1* plasmid for the expression of *SLK19-GFP* from its own promoter. The open reading frame (ORF) and 5′ promoter region were PCR amplified using pXZB10 as a template and the XbaI- and SalI-linked oligonucleotides CTCtctagaATTTACGCCGGGGG and GGGgtcgacGTTTTTTTTCATTTTCTAACAAC. The resulting 3793-bp PCR product was cut with XbaI and SalI and ligated into pJK52 (a plasmid encoding a fusion of the *NUF2* gene to the S65T; V163A mutant of GFP; Kahana et al., 1998), which had been cut with SpeI and XhoI. The resulting plasmid included 579 bp of the *SLK19* 5′ promoter region with the entire 2463-bp ORF fused to GFP and the *NUF2* 3′ untranslated region. pJK145 is a *URA3* integrating vector for the replacement of the endogenous *SLK19* gene with the *SLK19:GFP:NUF2 3′UTR* gene. A 2580-bp SacI/KpnI fragment encompassing a 3′ fragment of the *SLK19* ORF fused to GFP and the *NUF2* 3′ UTR was ligated into pRS306 (Sikorski and Hieter, 1989) that had been similarly cut.

KAR3–GFP Fusion Plasmids. pJK148 is a *CEN TRP1* plasmid for the expression of *KAR3–GFP* from its own promoter. The ORF and 5′ promoter region were PCR amplified using pMR798 (Meluh and Rose, 1990) as a template and the SpeI- and XhoI-linked oligonucleotides, GGGactagtAGAACCATCATCATG and GGctcgagCTTTTCTACTAACCAATCTGG. The resulting 2984-bp PCR product was cut with XhoI and SpeI and ligated into a similarly-cut pJK52 backbone. The resulting plasmid in-

cluded 699 bp of the *KAR3* 5′ promoter region with the entire 2187-bp ORF fused to GFP and the *NUF2* 3′ UTR. pJK152 is a *URA3* integrating vector for the replacement of the endogenous *KAR3* gene with the *KAR3–GFP:NUF2 3′UTR* gene. An 1809-bp XmnI/KpnI fragment encompassing a 3′ fragment of the *KAR3* ORF fused to GFP and the *NUF2* 3′ UTR was ligated into pRS306 (Sikorski and Hieter, 1989) that had been cut with SmaI and KpnI.

CBF2–GFP Fusion Plasmids. Plasmid pJK66 was constructed as a centromeric vector for the expression of *CBF2* fused to GFP. The *CBF2* promoter and ORF were amplified by PCR with the oligonucleotides CCggatccTGTCTGCTCAGCTAGTGG and CCctcgagCGTTAGATAGATATACTAAC. The PCR product was digested with BamHI and XhoI, and the GFP-Nuf2 3′UTR region was isolated by digesting pJK145 with KpnI and XhoI. These were ligated into the *CEN/LEU2* vector pRS315 that had been cut with BamHI and KpnI (partial digest). pJK66 was transformed into strain 316Bα. Cells transformed with pJK66 could become resistant to 5-FOA, signifying that *CBF2–GFP* could functionally complement the *cbf2*Δ lethality phenotype. pJK171 (integrating *CBF2–GFP*) was prepared by digesting pJK66 with XbaI and KpnI and ligating the 2.5-kb Cbf2p/GFP/Nuf2 3′ UTR truncation fragment into a similarly-cut pRS316.

Strain Construction

Strains were constructed as follows: strain JKY288 (*slk19::SLK19:GFP:URA3*), pJK145 was linearized with ClaI and transformed directly into strain JKY196; strain JKY292 (*kar3::KAR3:GFP:URA3*), pJK152 was linearized with HpaI and transformed directly into strain JKY196; strain JKY196 (*cbf2::CBF2:GFP:URA3*), pJK171 was linearized with HpaI and transformed into strain JKY196.

Live Cell Microscopy Techniques

Visualization of spindle pole bodies (SPBs) in live cells is based upon the technique of Kahana et al. 1998. Microscope growth chambers were prepared as follows: microscope slides were coated with 1 ml of molten SC-ura/2% agarose. Next, a second slide was placed on top, and the sandwich was allowed to cool to room temperature for 20 min. The top slide was removed, and 3 μl of cells from a logarithmic overnight culture were placed in the center of the solidified medium. A 22 × 22-mm number 1 1/2 cover slide was placed over the cells, and the remaining solid medium was cut away with a razor blade. Finally, the cover slip was sealed with molten VALAP (1:1:1 petroleum jelly:lanolin:paraffin) wax. During observations, the slides were maintained at 25°C using a thermostat-controlled heated microscope stage insert (Micro Video Inc.).

Observations were taken on a Nikon Diaphot 300 inverted microscope equipped with a 60× 1.4 N.A. Plan-Apo objective lens, a 100W Hg epifluorescence illuminator, and GFP filter set #41018 (Chroma Technology). Digital images were obtained using a CH250/KAF1400 cooled-CCD camera (Photometrics) that was controlled by the Metamorph 2.5 software (Universal Imaging). Cells were observed using 100 ms exposures taken every 10–30 s with manually-controlled motorized focusing. Fluorescence illumination was controlled by a Uniblitz shutter (Vincent Associates) that was synchronized with the camera shutter. For frame of reference, DIC images were acquired immediately before and after the fluorescence time-lapse series.

Results

slk19 Mutants Have Reduced Spindle Mts and Increased Cytoplasmic Mts

To identify novel proteins related to Kar3p in function, we performed a screen for mutants that require the Kar3p protein for viability. In short, a strain containing a deletion of the *KAR3* gene (*kar3*Δ) was transformed with a plasmid containing the wild-type *KAR3* and a negative selection marker *URA3*, the gene for orotidine-5′-phosphate decarboxylase (Boeke et al., 1984). Ura3p inhibits growth on 5-FOA, due to the synthesis of the toxic 5-fluorouracil. Without additional mutations, the *kar3* mutant can lose the *KAR3-URA3* plasmid (p*KAR3-URA3*), although it does so more slowly than wild-type cells. A synthetic-lethality screen was performed by mutagenizing *kar3*Δ p*KAR3-URA3* cells and selecting mutants unable to grow in the presence of 5-FOA. One such mutant and the *SLK19* locus were identified (as described in Materials and Methods).

The *SLK19* gene is locus YOR195w (*Saccharomyces* Genome Database). The protein (Slk19p) has a predicted molecular weight of 95,324 and is most likely highly charged with a predicted pI of 4.74. The protein secondary structure prediction program (BCM Search Launcher) suggests that much of the COOH terminus of Slk19p, ~600 amino acids, forms an α-helical rod domain. Slk19p also contains several potential leucine zipper regions, but all are missing a conserved basic region upstream (Alber, 1992).

We replaced a single copy of the *SLK19* ORF in a wild-type diploid yeast strain with the *HIS3* gene (*slk19*Δ) by homologous recombination (Baudin et al., 1993). *slk19*Δ/*SLK19* diploids sporulated four viable spores indicating that *SLK19* is not an essential gene. Correct integration of the *HIS3* gene at the *SLK19* locus was confirmed by crossing the deletion allele to the original *slk19* mutation and by comparing the deletion phenotypes with that of the original mutant (Materials and Methods).

To determine whether loss of Slk19p affects Mts or cell division, we examined *slk19* mutant cells by indirect immunofluorescence with antitubulin antibodies and the chromatin-binding dye DAPI. Loss of *SLK19* leads to an increase in mitotic cells (those with short bipolar spindles and a single nucleus) from ~20% in cultures of isogenic wild-type cells to slightly >40% in *slk19*Δ cultures (not shown). *slk19* mutants also have nuclear spindles that were ~33% shorter, and with roughly twice as many cytoplasmic Mts as wild-type strains (Fig. 1, A and B). Though short, these spindles remained bipolar, as shown by staining with antibodies to the SPB protein Spc90 (Fig. 1 B; antibodies courtesy of J. Kilmartin, MRC, Cambridge, UK). We found that 98% of the wild-type, 92% of *slk19*Δ, and 93% of the *kar3*Δ mutant cells with large buds and a single nucleus, had two spindle poles as shown by anti-Spc90 staining ($n = 100$ of each genotype). The spindle poles in the *slk19*Δ mutant were closer together than those of wild-type cells, consistent with a shorter spindle (Fig. 1 B). Thus, loss of *SLK19* causes a partial mitotic arrest or delay, and a shift in Mt density from the nucleus to the cytoplasm, with shorter spindles and more cytoplasmic Mts. This is similar to the *kar3* phenotype reported previously (Saunders et al., 1997a). Some differences between the *kar3*Δ and *slk19*Δ mutants were noted. The *slk19*Δ mutant had more cytoplasmic Mts, but they were not appreciably longer than in wild-type, whereas the *kar3*Δ mutant has both increased numbers and lengths of cytoplasmic Mts (Fig. 1, A and C). A second difference was that the *kar3*Δ mutant showed a marked increase in cytoplasmic Mt number upon cell cycle arrest with HU or mating pheromone (Saunders et al., 1997a), whereas the Mt arrays of arrested *slk19*Δ mutants where not distinguishable from unsynchronized *slk19*Δ cells at the same point of the cell cycle (not shown).

Slk19p Is Located at the Centromeres and the Spindle Midzone, Whereas Kar3p Is an SPB Component

Localization of Slk19p was determined by construction of

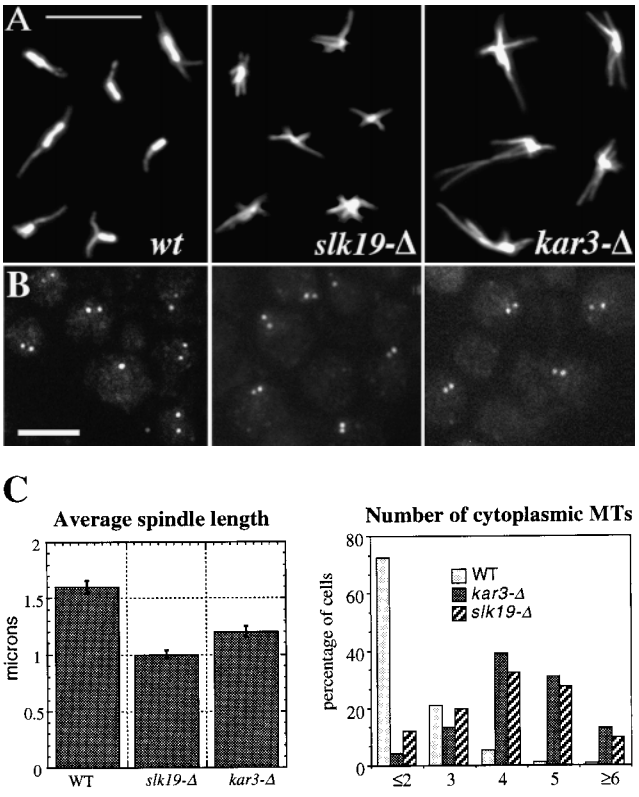

Figure 1. Mt phenotypes of *SLK19* mutants. (A) Disruption of *SLK19* leads to reduced spindle Mts and increased cytoplasmic Mts. Fixed cells were treated for antitubulin immunofluorescence (Materials and Methods). Spindles are visible as a bright fluorescent bar between fainter staining cytoplasmic Mts. To compare *kar3*Δ and *slk19*Δ mutants at the same point in the cell cycle, we imposed an HU arrest for 3.5 h. HU blocks progression through S phase, but in *S. cerevisiae*, allows spindle assembly (Mitchison and Carter, 1975). Shown is a composite image of representative cells from the same sample. Bar, 5 μm. (B) In a separate experiment, wild-type (wt), *slk19*Δ, and *kar3*Δ cells were arrested with HU for 3.5 h and immunostained with antibodies to the SPB protein, Spc90p (Rout and Kilmartin, 1990). Bar, 5 μm. (C) The lengths of 80 randomly picked spindles were measured and the numbers of cytoplasmic Mts for 400 randomly picked spindles from wild-type, *slk19*Δ, and *kar3*Δ cells were counted. SEM represented by error bars.

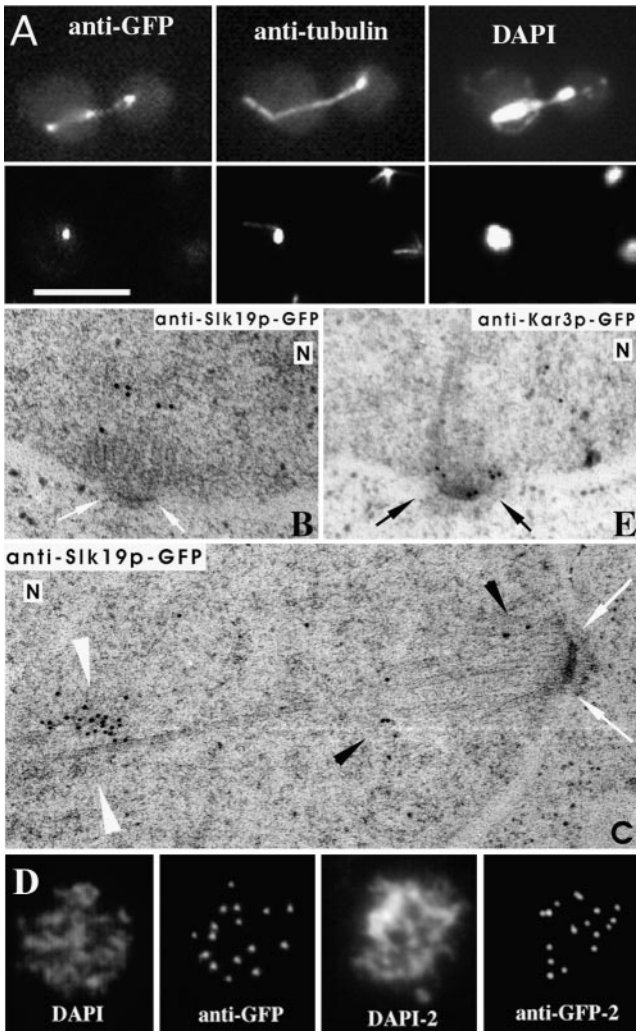

Figure 2. Immunolocalization of Slk19p–GFP and Kar3p–GFP fusion proteins. (A) Cells with *SLK19:GFP* integrated into the genome were fixed and stained with anti-GFP, antitubulin antibodies, and DAPI. The Slk19p is located on the spindle, near the poles, and at the spindle midzone of elongating spindles. Rarely, Slk19p staining can be seen along the length of the short spindle as shown. Bar, 5 μm. (B) Cells with integrated *SLK19:GFP* were treated for immunoelectron microscopy with antibodies to GFP. The white arrows point to the edges of the SPB and the nuclear side is labeled N. (C) The midzone cluster of Slk19p staining is shown on an elongated anaphase spindle. White arrowheads point to the midzone staining, black arrowheads to Slk19p at the poles, and white arrows to the edges of the SPB. (D) Chromosomal association of Slk19p. A diploid cell with homozygous integrated *SLK19:GFP* was grown in sporulation medium for 28 h. The cells were then spheroplasted to remove the cell wall, and lysed in low ionic strength solution. The lysate was allowed to attach to glass slides, fixed with paraformaldehyde, and stained with antibodies to GFP and with DAPI. Two examples are shown. (E) Immunoelectron microscopy localization of Kar3p. Cells with integrated *KAR3:GFP* were treated for immunoelectron microscopy with antibodies to GFP. The black arrows point to the edges of the SPB and the nuclear side is labeled N.

a *SLK19:GFP* hybrid gene (Materials and Methods), which fully complements the *slk19*Δ phenotype and the *slk19*Δ *kar3*Δ synthetic lethality (not shown). To avoid misleading results from variation in plasmid copy number, all experimental results shown are with the *SLK19–GFP* gene fusion integrated into the genome, inactivating the endogenous *SLK19* gene. For the purposes of localization of Slk19p, both live and fixed cells stained with anti-GFP antibodies were examined. To establish the position of the GFP relative to the spindle Mts, fixed cells were treated for immunofluorescence with both anti-GFP and antitubulin antibodies (Fig. 2 A). Slk19p–GFP was observed in the vicinity of the single SPB of unbudded cells (not shown) and at both SPBs of G2/M cells. In addition, a minority of the preanaphase cells had Slk19p staining along the length of spindles. In anaphase cells, Slk19p–GFP fluorescence was also observed at the approximate midzone of the spindles, typically as a single dot, but occasionally as a smear of staining in the middle of the spindle. Labeling of cytoplasmic Mts was never observed.

To further define the position of the Slk19p in the spindle, Slk19p–GFP was localized by immunoelectron microscopy using anti-GFP antibodies. This analysis revealed that Slk19p is not a true SPB component. Rather, the immunostaining was associated with Mts and was clustered around the SPBs (Fig. 2 B). In anaphase cells, Slk19p spindle midzone immunostaining could also be seen by EM, but no distinctive spindle structure was visible at this site (Fig. 2 C).

The immunoelectron microscopy localization of Slk19p–GFP is suggestive of chromosomal association. Chromosomes are known to associate with spindle poles through much of the cell cycle in *S. cerevisiae* (Guacci et al., 1997). Thus, to determine whether Slk19p is indeed chromosome-associated, we performed a meiotic chromosome squash experiment (Loidl et al., 1998). *SLK19-GFP* cells were grown in sporulation medium for 28 h, treated with Zymolyase (USBiological) to remove the cell wall, and lysed in the presence of detergent under low osmotic conditions on glass slides. These preparations were stained with antibodies to GFP and counterstained with DAPI. Anti-GFP staining from cells without Slk19p–GFP, or without primary antibody, was uniformly negative (not shown). With anti-GFP-Slk19p staining, we observed dots of immunofluorescence on the chromatin (Fig. 2 D). This staining pattern was quite variable from spread to spread on the same slide. We have attempted to objectively quantify the number of fluorescent dots by finding examples of well preserved chromatin, as judged by the DAPI staining, then counting the dots in the rhodamine-fluorescence channel used to visualize the anti-GFP-Slk19p staining. In 100 samples, we observed 15% of the spreads with 1–5 dots of anti-GFP-Slk19p staining, 40% with 6–10 dots, and 45% with 11–16 dots. More than 16 separate dots, the number of centromeres in *S. cerevisiae*, was never observed, although some dots appeared as doublets (Fig. 2 D, right). We interpret these results to indicate that during meiosis, Slk19p is chromosome-associated and apparently present at a single element on each chromosome.

The only known single chromosomal elements are centromeres. To test for centromere association, we determined whether Slk19p could be cross-linked to centromere DNA through a chromatin immunoprecipitation assay (ChIP; Meluh and Koshland, 1997). *SLK19-GFP* cells were treated with 1% formaldehyde to cross-link Slk19p–GFP to any associated chromatin. Cell extracts were immunoprecipitated with anti-GFP antibodies, and coimmunoprecipitated DNA was analyzed by PCR using primers specific to centromeric or noncentromeric DNA sequences (Fig. 3). For extracts from cells with integrated *SLK19-GFP*, primers complementary to the centromeric loci from chromosomes III and XVI gave a much stronger signal than those complementary to the noncentromeric loci *ARS2* and *MET2*, indicating that Slk19p preferentially cross-links to centromeric DNA (Fig. 3 A; a single weak band was visible for both noncentromere primers that we could not reproduce when we made copies for publication).

Both Kar3p and Slk19p have similar mutant phenotypes and are synthetically lethal, suggesting they may act in functionally related pathways. Furthermore, previous studies have implicated Kar3p as a kinetochore protein

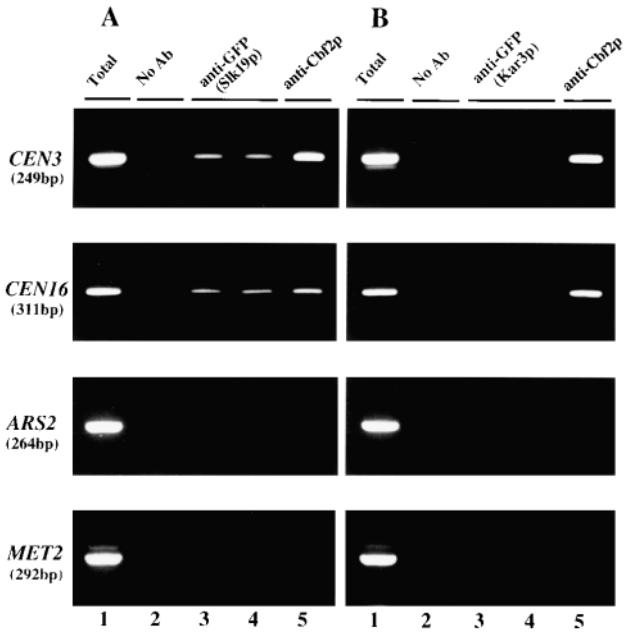

Figure 3. Coimmunoprecipitation of *CEN* DNA and Slk19p–GFP. Cross-linked chromatin was prepared from strains WSY990, integrated *SLK19:GFP* (A); and JKY292, integrated *KAR3:GFP* (B), and then immunoprecipitated with no antibody (lane 2), anti-GFP (lanes 3 and 4, performed in duplicate), or anti-Cbf2p antibodies (lane 5). Total input DNA (lane 1) and coimmunoprecipitated DNA were analyzed by PCR using primers specific to *CEN3, CEN16, ARS2, or MET2* (Materials and Methods). The PCR products were run on 2% agarose gels and stained with ethidium bromide. Sizes of the PCR products are shown in parentheses.

through its involvement in CEN DNA coated bead-Mt attachment in vitro (Middleton and Carbon, 1994). To confirm that Kar3p is also found at centromeres, we constructed a *KAR3–GFP* hybrid gene that compliments the *kar3* mutational phenotype for karyogamy and allows viability of the *slk19 kar3* mutant combination (not shown). Cells with integrated *KAR3–GFP* were tested for centromere-association of *KAR3–GFP* by the ChIP assay. Surprisingly, we found no evidence for a Kar3p centromere association in vivo (Fig. 3 B). Furthermore, when this strain was tested by immunoelectron microscopy analysis, Kar3p-GFP was not clustered around the poles, as was Slk19p, but was closely associated with the nuclear side of the SPB (Fig. 2 E). We interpret these results to indicate that Slk19p is associated with centromeric DNA, whereas Kar3p is predominantly associated with the nuclear face of the SPB.

Either Kar3p or Slk19p Is Required to Stabilize the Spindle

To examine the consequence of concurrent loss of both Slk19p and Kar3p, a ts allele of *KAR3* (*kar3-ts*) was synthesized by PCR mutagenesis. This allele supported growth of the *slk19*Δ *kar3*Δ mutant at 26°C, but not at 34°C (Materials and Methods). *slk19*Δ *kar3*Δ cells with *kar3-ts* on a plasmid (p*kar3-ts*) were grown to log phase at

26°C and shifted to 35°C for 3 h to inactivate Kar3p. After the temperature shift, the cells showed a severe G2/M arrest, with >80% of the cells having a large bud and a single undivided nucleus (Fig. 4 A). When temperature-shifted cells were fixed and stained for indirect immunolabeling of Mts, it was apparent that the cells were unable to assemble or maintain a spindle in the absence of Slk19p and Kar3p, as most cells had a monopolar Mt array (Fig. 4 B). To confirm a monopolar structure, we also stained cells with antibodies to the SPBs (Fig. 4 C). Before the temperature shift, 46% of the *slk19*Δ cells had only one site of spindle pole staining, but, after shifting to 35°C for 3 h, 90% had only a single site of staining (n = 100 for each genotype), confirming a monopolar arrest of these cultures.

Next, we investigated whether the Kar3p and Slk19p proteins were essential for progression through the cell cycle after spindle assembly. *slk19*Δ *kar3*Δ p*kar3-ts* cells were arrested with preassembled spindles by blocking DNA replication with HU at 26°C. When released at 26°C, the mutants underwent anaphase, but at 35°C, when Kar3p is inactive, division was blocked, as determined by the persistence of large budded cells with a single nucleus (not shown). To investigate the nature of the mitotic arrest, cells were stained with antibodies to both Mts and the SPB protein Spc90p (Fig. 5 A). Under these double labeling conditions, the spindle Mts can readily be identified as the Mts between the immunostained spindle poles. The spindles in the *kar3*Δ *slk19*Δ mutants rapidly disappeared and were mostly missing within 20 min of the temperature shift. It was apparent that the spindles were collapsing in the double mutant, as shown by the convergence of the two SPBs (Fig. 5 A). After the spindles dissociated, the cytoplasmic Mts began to grow in length and number in these arrested mutants. In both synchronized and log phase cultures, elongating anaphase spindles were resistant to collapse (not shown). We determined the frequency of spindle collapse in HU arrested *kar3*Δ *slk19*Δ mutants by counting the numbers of cells with one visible SPB, two separated SPBs, or two adjacent SPBs, as determined by anti-Spc90p immunolabeling (Table II). Before the temperature shift, most of the arrested cells had spindles with separated spindle poles; after the shift to 35°C, most of the spindles showed a collapsed phenotype, with only a single point of spindle pole staining or adjacent points of staining. These results indicate that either Kar3p or Slk19p must be present to maintain preanaphase spindle bipolarity.

Slk19p Is Left Behind at the Spindle Midzone as the Spindle Poles Separate in Anaphase B

As Slk19p appears to be a centromere protein, we were interested in the origin of the spindle midzone staining during anaphase B, when centromeres are not found at the

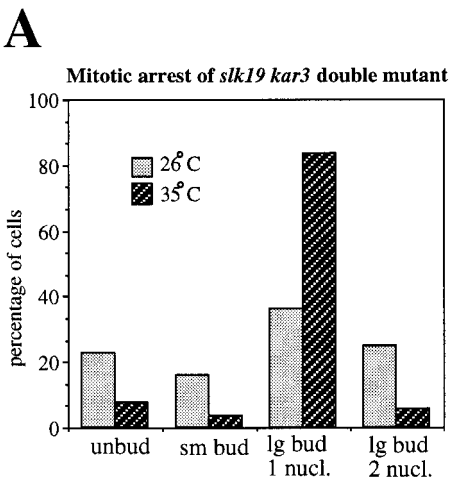

Figure 4. Loss of function of both *KAR3* and *SLK19* in the same cell leads to a severe mitotic arrest as large budded cells with a single nucleus. (A) The strain *kar3*Δ *slk19*Δ p*kar3-ts* was grown to log phase at 26°C and then switched to 35°C for 3 h. The cell cycle arrest was monitored by DAPI staining after 70% ethanol fixation. Arrest in G2/M was indicated by an increase in the number of cells with a large bud and a single nucleus. 300 randomly picked cells were counted. (B) The *kar3*Δ *slk19*Δ p*kar3-ts* cells at 35°C from A were fixed and treated for antitubulin immunofluorescence and DAPI staining. (C) In a separate experiment, *kar3*Δ *slk19*Δ p*kar3-ts* cells grown at 35°C for 3 h were immunostained with antibodies to the SPB protein, Spc90p (Rout and Kilmartin, 1990). Bar, 5 μm.

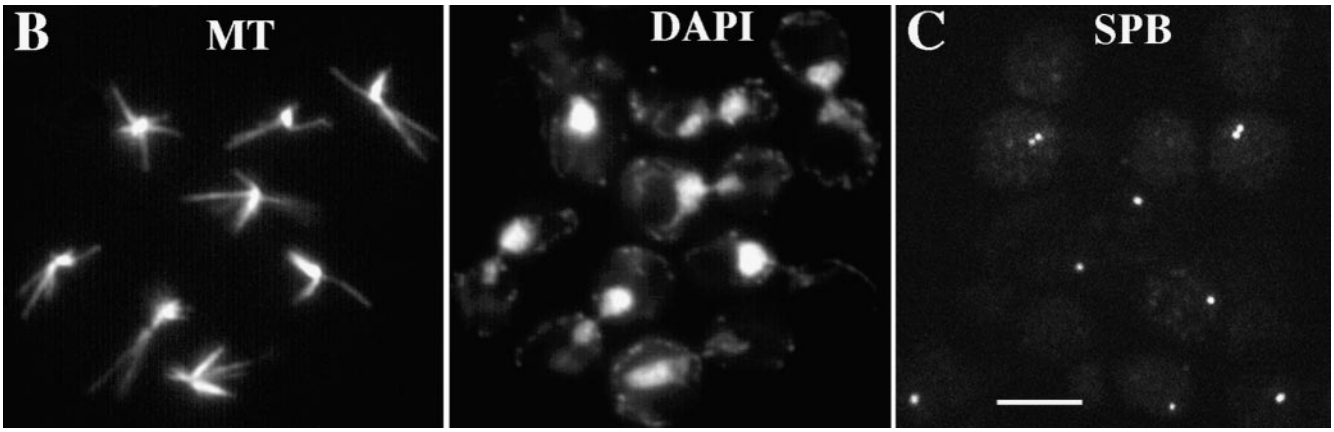

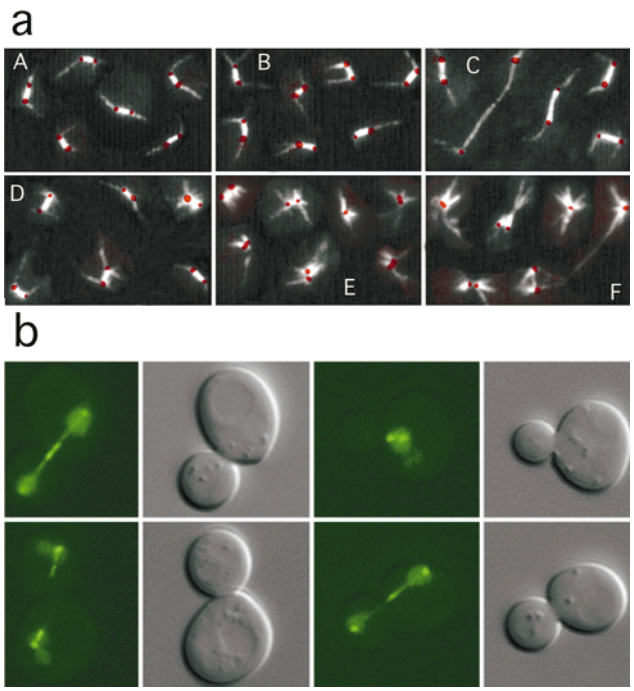

Figure 5. (a) Spindle collapse in the *slk19 kar3* double mutant. *slk19*Δ *kar3*Δ p*kar3-ts* and control cells were arrested in YEPD with 0.1 M HU for 3.5 h. The cells were then transferred to 35°C while still in HU. After 20 min at 35°C, the cells were resuspended in fresh medium without HU at 35°C, and returned to a shaking water bath at 35°C. At the selected times, cells were fixed and stained with antibodies to tubulin (white) and spindle poles (red). A, B, and C are wild-type cells; D, E and F are *slk19*Δ *kar3*Δ p*kar3-ts* mutants. Total time at 35°C is: 0 min, A and D; 20 min, B and E; and 100 min, C and F. (b) Cbf2p–GFP is found at the spindle midzone. A *CBF2:GFP* hybrid gene was integrated into a wild-type genome and the position of the fusion protein in live cells recorded. The staining was similar to that reported previously in fixed cells (Goh and Kilmartin, 1993), except that additional labeling at the spindle midzone also was noted. GFP is shown in green and the corresponding DIC image on its right.

midzone of the spindle by fluorescence in situ hybridization analysis (Guacci et al., 1997). At the beginning of anaphase, we observed Slk19p–GFP fluorescence as two dots; however, one of them was typically brighter than the other (Fig. 6 A). Shortly after cells entered anaphase B, the staining from the brighter pole could be seen to divide into two parts as the spindle elongated (Fig. 6 A, arrow, first seen at 30 s). The middle staining region marked the midzone of the spindle. The midzone staining remained visible throughout most of anaphase, and was typically lost shortly before spindle disassembly (as determined by noncoordinated movements of the poles). The appearance of the midzone Slk19p–GFP staining was observed in all eight recorded anaphases. The midzone staining could be detected as arising from a single spindle pole in six of the eight anaphases. In the remaining two, the origin of the midzone staining could not be determined. The midzone staining arose from the spindle pole destined for the bud in three of the six, and for the mother in three of six divisions, showing that the midzone staining could arise from either pole. In five of six examples, the spindle pole that

Table II. Spindle Collapse in slk19 kar3 Mutants

	Separated SPBs	Adjacent SPBs	Single visible SPB
	%	%	%
slk19 kar3 26°C	87	8	5
slk19 kar3 35°C	15.5	32.5	52
wild-type 35°C	95	3	2
wild-type 26°C	96	3	1

The indicated strains were arrested with 0.1 M HU at 26°C for 3.5 h and then switched to 35°C for 20 min (still in the presence of HU). Samples were taken before and after the temperature switch for immunofluorescence with anti-SPB and antitubulin antibodies. A total of 100–200 cells were counted. Note that a single point of SPB staining can be either a single SPB or two SPBs that are too close together to resolve as separate structures. The experiment was repeated once with similar results.

would give rise to the midzone staining was visibly brighter with GFP fluorescence than the other pole. The change in position of the three staining regions of Slk19p–GFP with time in a single anaphase is shown in Fig. 6 B. The pole–pole separation represents the distance between the clustered kinetochores at the poles. The dim pole–center and bright pole–center lines are the distances between the poles and the center staining region. The bright pole is the one that gave rise to midzone staining. As the spindle poles separated, the change in distance from the poles to the midzone regions was the same for both poles. This indicates that the midzone region is in fact remaining stationary within the spindle while the poles move away isometrically, leaving the new GFP-labeled staining in the approximate midzone of the spindle, offset by the original length of the spindle.

To determine whether the midzone spindle staining could also be seen with other kinetochore proteins, we constructed a functional GFP-tagged hybrid of *CBF2* (*NDC10/CTF14/CEP2*), a component of the centromere-binding CBF3 complex (Goh and Kilmartin, 1993; Jiang et al., 1993). As observed previously in fixed cells (Goh and Kilmartin, 1993), Cbf2p-GFP was associated with the spindle poles, but we also observed staining of the midzone region of the late anaphase spindle (Fig. 5 B). This observation suggests that other centromeric proteins in yeast may also be found in the spindle midzone in the absence of centromeres. Note that Cbf2p-GFP exhibited diffuse nuclear fluorescence, making the movement in real-time difficult to document.

slk19 Mutants Are Inviable in the Absence of Kar3p and Cin8p

To determine whether Slk19p is required in the absence of other Mt-based motors besides Kar3p, we examined whether the *slk19*Δ mutation was lethal in *kip1, kip2, kip3, cin8,* or *dyn1/dhc1* mutant backgrounds. All combinations of double mutants were readily isolated, with the exception of *cin8*Δ *slk19*Δ (not shown). *cin8*Δ *slk19*Δ mutants were also unable to lose *CIN8* on a plasmid (Fig. 7 A), and when the *slk19* mutant was crossed to a *cin8-3* ts allele, the double mutant was more ts than the *cin8-3* strain alone (Fig. 7 B). These results indicate that *slk19*Δ mutants also cannot survive without *CIN8.* Note that the *cin8-3 slk19*Δ double mutant did not show a uniform cell cycle arrest at the nonpermissive temperature and retained spindle structure. The nature of the lethality is not known. Each of the

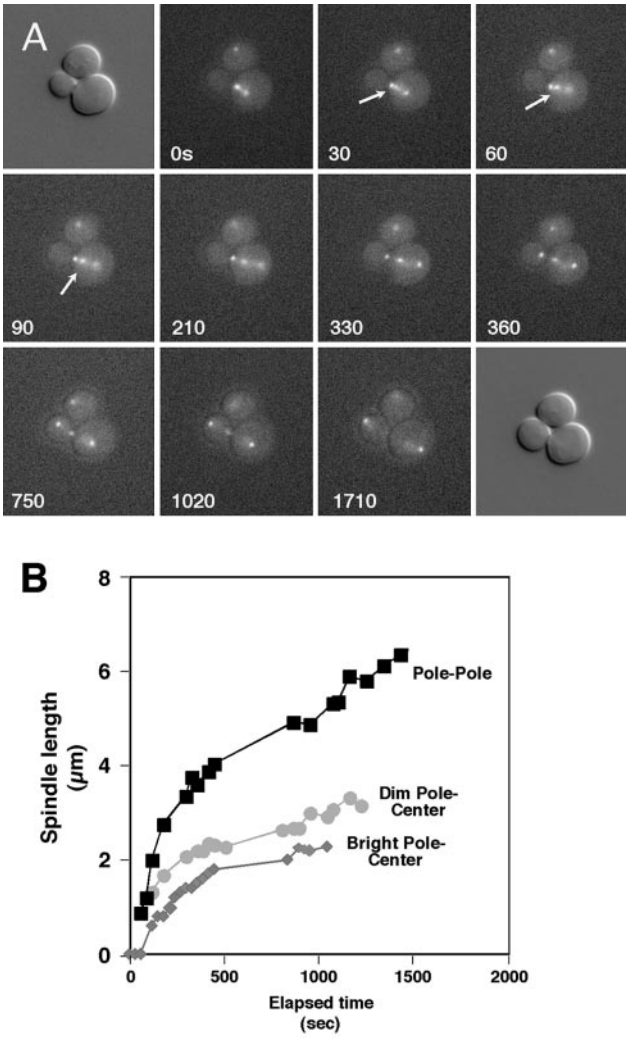

Figure 6. Slk19p–GFP movement in live cells. (A) Cells were visualized by epifluorescence microscopy at the indicated times. Time zero is an arbitrary starting point. Arrows indicate the origin of the third spot of Slk19–GFP staining. The starting and ending DIC images are shown. Growth of the bud indicates these cells remain viable over the recorded time period. (B) The distances between the two poles, brighter pole and center spot, and dimmer pole and center spot of Slk19-GFP fluorescence are shown for a single anaphase cell. The measurements were made twice with similar results.

mitotic motor mutants in *S. cerevisiae* has a unique synthetic lethal profile with mutations in the other Mt motors (a partial list is given in Cottingham and Hoyt, 1997). None of these synthetic lethal profiles fit that of *slk19*Δ, implying that Slk19p is not an essential component of any of the mitotic motor pathways.

Previously, *kar3*Δ mutants have been shown to grow better in the presence of drugs, such as benomyl, that stimulate Mt depolymerization (Roof et al., 1991; Saunders et al., 1997a). We also investigated whether benomyl suppressed the *slk19*Δ phenotype. Because the *slk19* single mutants have high viability, we examined the effect of benomyl on *slk19 kar3* double mutants. *slk19*Δ *kar3*Δ p*kar3-ts* cells were plated on YEPD, with or without the addition of 5 μg/ml benomyl. Benomyl allowed the double mutant to grow at 34°C, indicating that this Mt inhibitor could partially suppress the *slk19 kar3* synthetic lethality (Fig. 7 B). Notably, benomyl was also able to rescue the synthetic lethality of both *dhc1*Δ *kar3*Δ p*kar3-ts* (Fig. 7 B) and *kip3*Δ *kar3*Δ p*kar3-ts* strains (not shown), supporting the hypothesis that an excess of Mts is a major cause of the *kar3*Δ-associated phenotypes (Saunders et al., 1997a). Benomyl also allowed the growth of *cin8-3 slk19*Δ double mutants at the nonpermissive temperature, indicating that this Mt inhibitor could partially suppress the *slk19*Δ phenotype, as well as the *kar3*Δ phenotype. A deletion of the *KIP2* motor, which causes a marked reduction in cytoplasmic Mts (Cottingham and Hoyt, 1997; Huyett et al., 1998), however, did not allow growth of the *slk19*Δ *kar3*Δ p*kar3-ts* cells at 34°C in the absence of benomyl (Fig. 7 B). These results indicate that the inviability from loss of both Kar3p and Slk19p could not be entirely prevented by a reduction in cytoplasmic Mt numbers.

Discussion

We have identified a gene that is required in the absence of the kinesin motor Kar3p. While Slk19p–GFP is present during most of the cell cycle in the vicinity of the SPBs, we believe that Slk19p is a centromere protein based on three assays. First, by immunoelectron microscopy, the protein was associated with nuclear Mts near the spindle poles, but was absent from the SPB. Yeast kinetochores are known to associate with the spindle poles during most of the cell cycle (Guacci et al., 1997). Second, during meiosis, Slk19p is visible at a single site on the chromosomes. Third, the ChIP assay indicates that Slk19p can be preferentially cross-linked to the centromere DNA. So, while Slk19p is usually observed at the poles of preanaphase spindles, we believe this represents a poleward clustering of centromeres.

While the Slk19p protein appears to associate with centromeres, not all Slk19p is present at this position. At the start of anaphase, a third site of Slk19-GFP fluorescence appears within the spindle at the midzone. This additional fluorescence at first is associated with one spindle pole, which is brighter than the second pole. When anaphase begins and the poles separate, the brighter pole leaves some of the Slk19p–GFP behind at the spindle midzone. After separation, the brighter pole exhibits the same fluorescence intensity as the second pole. Our positional analysis shows that the midzone region, as defined by Slk19p–GFP, remains stationary on the spindle as both poles move away. We believe that one interpretation of these results is that Slk19p is also associated with the plus ends of polar Mts, and that these ends are asymmetrically distributed on the spindle. In *S. cerevisiae* there are relatively few polar Mts, an average of ten for the shortest class of spindles, and a large amount of heterogeneity in the position of the plus ends (Winey et al., 1995). In some cases, the plus ends tend to be clustered near one spindle pole (Winey et al., 1995, Figure 5, Nos. 5, 7, and 8), which we believe may give rise to the asymmetric immunolabeling of Slk19p–GFP at the poles. If the preanaphase B spindle is initially asymmetric (i.e., the midzone region clustered near a pole), then one would expect to see one bright pole (due to the

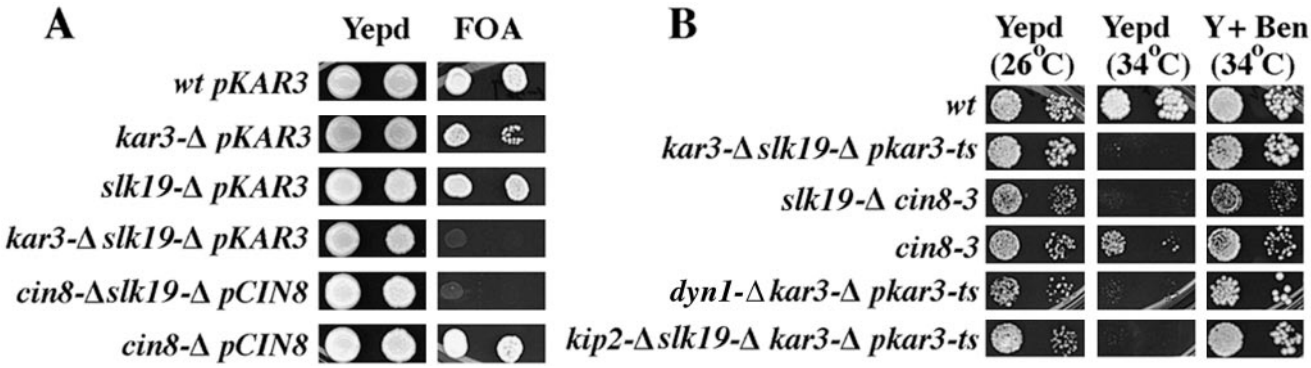

Figure 7. Synthetic lethality of *kar3*Δ *slk19*Δ and *cin8*Δ *slk19*Δ combinations. (A) The indicated strains were transformed with plasmids containing *URA3* and *CIN8* or *KAR3,* and plated onto YEPD and 5-FOA plates at 30°C for 2 d. (B) Benomyl, but not a *KIP2* deletion, could suppress the growth defect of *kar3* and *slk19* mutants. The strains were plated onto YEPD plates at 26°C or 34°C (except *dyn1*Δ *kar3*Δ *pkar3-ts*, which requires 35°C to show an effect of benomyl) for 48 h with (Y + Ben) or without 5 μg/ml benomyl. wt, wild-type.

16 chromosomes + the midzone signal) and one dim pole (with 16 chromosomes) at the onset of anaphase. Consistent with our observations, spindle elongation during anaphase B would cause the midzone fluorescence to appear to emerge from the bright pole. Equal rates of polymerization from each side would cause the midzone to remain slightly off center throughout anaphase, as observed. Thus, we believe that the continued association of Slk19p with the spindle midzone may reflect an affinity for the plus ends of polar Mts. Further analysis will be required to determine if Slk19p binds directly to the Mt ends.

The phenotype of *slk19* mutants is a shift of Mt density from the nucleus to the cytoplasm. In *slk19 kar3* double mutants, the spindle collapses completely. We interpret the spindle collapse to be a consequence of the spindles becoming too small to support bipolarity. Thus, Slk19p appears to function to stabilize the spindle, and more specifically spindle Mts. We propose that Slk19p functions at the plus ends of Mts, both at the centromere and also the ends of polar Mts, to stabilize them from depolymerization. Polar Mts in metaphase animal cells are much less stable then k-Mts, but once spindle elongation begins, the polar Mts must elongate substantially to support anaphase B (Masuda and Cande, 1987). In *S. cerevisiae*, the spindle increases in length nearly eightfold (Byers, 1981; Winey et al., 1995), presumably involving an increase in stability of the polar Mts at this time.

The spindle phenotype from loss of *slk19* is similar to the effect of removing the chromosomes from animal cells. In grasshopper spermatocytes, removal of all the chromosomes from a metaphase cell resulted in a ~60% loss of Mt birefringence (Zhang and Nicklas, 1995). Like *slk19* mutants, the chromosomeless spindles were able to complete a normal anaphase B. We suggest that both these micromanipulation experiments and the genetic deletion of *SLK19* are analogous, in that they both eliminate the stabilizing influence of chromosomes on spindle Mts.

While Slk19p is found at the kinetochores, it may not have a role in chromosome attachment. The *slk19*Δ mutant grows normally and does not show the inviability associated with chromosome loss in mitosis or meiosis. There is only a single k-Mt per chromosome in *S. cerevisiae* (Winey et al., 1995). If the reduction in spindle length was from loss of centromere attachment and subsequent destabilization of the k-Mt, chromosome missegregation should be very high and cell viability low. Also, Slk19p is not required for the Mt binding of the yeast centromere CBF3 complex (Severin, F., and A. Hyman, unpublished observations), and Slk19 mutants lose CEN plasmids at approximately the same frequency as wild-type strains (Zeng, X., and W. Saunders, unpublished observations). Therefore, the *slk19* phenotype suggests that the two centromeric functions, Mt stabilization and chromosome attachment, may be separable. Since chromosomes can hold on to the ends of both growing and shrinking Mts, the mechanisms controlling attachment and polymerization might be expected to be different.

Our analysis of Cbf2p-GFP shows that this centromere protein can also be found at the spindle midzone in anaphase B. A variety of kinetochore proteins in animal cells are known to associate with the spindle midzone and resulting midbody. These include the Mt motors CENP-E, dynein, and CHO1, and the nonmotor proteins, CENP-F and INCENPs (Cooke et al., 1987; Yen et al., 1991; Rattner et al., 1993; Karki et al., 1998). The function of kinetochore proteins in the midzone is generally unknown, but they have been proposed to play a role in cytokinesis or anaphase B. We propose that the plus ends of polar Mts may have a complex of proteins related to those that associate with the kinetochores. Kinetochore proteins were originally defined with the use of autoimmune sera and these autoantigens are mostly confined to the kinetochore (Earnshaw and Rothfield, 1985). As more kinetochore proteins become identified by other means, we may find that they do not all have the same distribution as the autoimmune antigens, but also form a complex at the plus ends of polar Mts.

While the *slk19* mutant spindle gets shorter, the cytoplasmic Mts get more numerous. The increase in cytoplasmic Mt numbers observed in the *slk19*Δ mutants may be an indirect effect of depolymerization of the spindle Mts. Slk19p was not found on cytoplasmic Mts, and the marked increase in cytoplasmic Mts in the *kar3*Δ *slk19*Δ double mutant is subsequent to the loss of the spindle. It is possi-

ble that the growth of the cytoplasmic Mts may be an indirect consequence of the depolymerization of the polar Mts. This may explain the suppression of the *slk19 kar3* and *slk19 cin8* growth defects by the Mt inhibitor benomyl. Cytoplasmic Mts are more sensitive to benomyl than nuclear Mts, and at the appropriate concentration, benomyl may preferentially force depolymerization of the cytoplasmic Mts, thus restoring spindle Mt integrity. However, deletion of *KIP2*, which leaves very few cytoplasmic Mts, does not allow growth of the *slk19 kar3* mutants, and the relationship between the growth of the cytoplasmic Mts and the loss of spindles is unclear.

The authors would like to acknowledge useful discussions with Drs. Jeffrey Brodsky and Charles Walsh at the University of Pittsburgh, and Dr. Donald Cleveland at the Ludwig Institute (UCSD). We would also like to thank Dr. John Kilmartin for the anti-SPB antibodies.

This manuscript was made possible by funding support from the American Cancer Society award CB-171 to W.S. Saunders, National Institutes of Health award RR0592 to J.R. McIntosh, and a Barr Investigator award to P.A. Silver.

Submitted: 11 February 1999
Revised: 17 June 1999
Accepted: 21 June 1999

References

Alber, T. 1992. Structure of the leucine zipper. *Curr. Opin. Genet. Dev.* 2:205–210.

Baudin, A., O. Ozierkalogeropoulos, A. Denouel, F. Lacroute, and C. Cullin. 1993. A simple and efficient method for direct gene deletion in *Saccharomyces cerevisiae*. *Nucleic Acids Res.* 21:3329–3330.

Boeke, J.D., F. LaCroute, and G.R. Fink. 1984. A positive selection for mutants lacking orotidine-5′-phosphate decarboxylase activity in yeast: 5-fluoroorotic acid resistance. *Mol. Gen. Genet.* 197:345–346.

Brinkley, B.R., and J. Cartwright, Jr. 1975. Cold-labile and cold-stable microtubules in the mitotic spindle of mammalian cells. *Ann. NY. Acad. Sci.* 253: 428–439.

Byers, B. 1981. Cytology of the yeast life cycle. *In* The Molecular Biology of the Yeast *Saccharomyces*: Life Cycle and Inheritance. J.N. Strathern, E.W. Jones, and J.R. Broach, editors. Cold Spring Harbor Laboratory Press, Cold Spring Harbor, NY. 59–96.

Cassimeris, L., C.L. Rieder, G. Rupp, and E.D. Salmon. 1990. Stability of microtubule attachment to metaphase kinetochores in PtK_1 cells. *J. Cell Sci.* 96:9–15.

Cooke, C.A., M.M. Heck, and W.C. Earnshaw. 1987. The inner centromere protein (INCENP) antigens: movement from inner centromere to midbody during mitosis. *J. Cell Biol.* 105:2053–2067.

Cottingham, F.R., and M.A. Hoyt. 1997. Mitotic spindle positioning in *S. cerevisiae* is accomplished by antagonistically acting microtubule motor proteins. *J. Cell Biol.* 138:1041–1053.

Desai, A., S. Verma, T.J. Mitchison, and C.E. Walczak. 1999. Kin I kinesins are microtubule-destabilizing enzymes. *Cell.* 96:69–78.

Ding, R., R.R. West, D.M. Morphew, B.R. Oakley, and J.R. McIntosh. 1997. The spindle pole body of *Schizosaccharomyces pombe* enters and leaves the nuclear envelope as the cell cycle proceeds. *Mol. Biol. Cell.* 8:1461–1479.

Earnshaw, W.C., and N. Rothfield. 1985. Identification of a family of human centromere proteins using autoimmune sera from patients with scleroderma. *Chromosoma.* 91:313–321.

Endow, S., S. Kang, L. Satterwhite, M. Rose, V. Skeen, and E. Salmon. 1994. Yeast Kar3 is a minus-end microtubule motor protein that destabilizes microtubules preferentially at the minus ends. *EMBO (Eur. Mol. Biol. Organ.) J.* 13:2708–2713.

Goh, P., and J.V. Kilmartin. 1993. NDC10: a gene involved in chromosome segregation in *Saccharomyces cerevisiae*. *J. Cell Biol.* 121:503–512.

Guacci, V., E. Hogan, and D. Koshland. 1997. Centromere position in budding yeast: evidence for anaphase A. *Mol. Biol. Cell.* 8:957–972.

Holy, T.E., and S. Leibler. 1996. Dynamic instability of microtubules as an efficient way to search in space. *Proc. Natl. Acad. Sci. USA.* 91:5682–5685.

Hoyt, M.A., L. He, K.K. Loo, and W.S. Saunders. 1992. Two *Saccharomyces cerevisiae* kinesin-related gene-products required for mitotic spindle assembly. *J. Cell Biol.* 118:109–120.

Huyett, A., J. Kahana, P. Silver, X. Zeng, and W. Saunders. 1998. The Kar3p and Kip2p motors function antagonistically at the spindle poles to influence cytoplasmic microtubule numbers. *J. Cell Sci.* 111:295–301.

Jiang, W., J. Lechner, and J. Carbon. 1993. Isolation and characterization of a gene (*CBF2*) specifying a protein component of the budding yeast kinetochore. *J. Cell Biol.* 121:503–512.

Kahana, J.A., G. Schlenstedt, D.M. Evanchuk, J.R. Geiser, M.A. Hoyt, and P.A. Silver. 1998. The yeast dynactin complex is involved in partitioning the mitotic spindle between mother and daughter cells during anaphase B. *Mol. Biol. Cell.* 9:1741–1756.

Karki, S., B. LaMonte, and E.L. Holzbaur. 1998. Characterization of the p22 subunit of dynactin reveals the localization of cytoplasmic dynein and dynactin to the midbody of dividing cells. *J. Cell Biol.* 142:1023–1034.

Kassir, Y., and G. Simchen. 1991. Monitoring meiosis and sporulation in *Saccharomyces cerevisiae*. *Methods Enzymol.* 194:94–110.

Loidl, J., F. Klein, and J. Engebrecht. 1998. Genetic and morphological approaches for the analysis of meiotic chromosomes in yeast. *Methods Cell Biol.* 53:257–285.

Manning, B.D., J.G. Barrett, J.A. Wallace, H. Granok, and M. Snyder. 1999. Differential regulation of the Kar3p kinesin-related protein by two associated proteins, Cik1p and Vik1p. *J. Cell Biol.* 144:1219–1233.

Masuda, H., and W.Z. Cande. 1987. The role of tubulin polymerization during spindle elongation. *Cell.* 49:193–202.

Meluh, P.B., and M.D. Rose. 1990. *KAR3*, a kinesin-related gene required for yeast nuclear fusion. *Cell.* 60:1029–1041.

Meluh, P.B., and D. Koshland. 1997. Budding yeast centromere composition and assembly as revealed by in vivo cross-linking. *Genes Dev.* 11:3401–3412.

Middleton, K., and J. Carbon. 1994. *Kar3*-encoded kinesin is a minus-end-directed motor that functions with centromere binding proteins (CBF3) on an *in vitro* yeast kinetochore. *Proc. Natl. Acad. Sci. USA.* 91:7212–7216.

Mitchison, J.M., and B.L. Carter. 1975. Cell cycle analysis. *Methods Cell Biol.* 11:201–219.

Mitchison, T.J., and M.W. Kirschner. 1985. Properties of the kinetochore *in vitro*. II. Microtubule capture and ATP dependent translocation. *J. Cell Biol.* 101:766–777.

Mitchison, T.J., L. Evans, E. Schultze, and M.W. Kirschner. 1986. Sites of microtubule assembly and disassembly in the mitotic spindle. *Cell.* 45:515–527.

Nicklas, R.B., and D.F. Kubai. 1985. Microtubules, chromosome movement, and reorientation after chromosomes are detached from the spindle by micromanipulation. *Chromosoma.* 92:313–324.

Page, B.D., L.L. Satterwhite, M.D. Rose, and M. Snyder. 1993. Localization of the *KAR3* kinesin heavy chain-like protein requires the *CIK1* interacting protein. *J. Cell Biol.* 124:507–519.

Pringle, J.R., A.E.M. Adams, D.G. Drubin, and B.K. Haarer. 1991. Immunofluorescence methods for yeast. *Methods Enzymol.* 194:565–602.

Rattner, J.B., A. Rao, M.J. Fritzler, D.W. Valencia, and T.J. Yen. 1993. CENP-F is a .ca 400 kDa kinetochore protein that exhibits a cell-cycle dependent localization. *Cell Motil. Cytoskelet.* 26:214–226.

Rieder, C.L. 1981. Effect of hypothermia (20–25 degrees C) on mitosis in PtK_1 cells. *Cell Biol. Int. Rep.* 5:563–573.

Roof, D.M., P.B. Meluh, and M.D. Rose. 1991. Multiple kinesin-related proteins in yeast mitosis. *Cold Spring Harbor Symp. Quant. Biol.* 56:693–703.

Rout, M.P., and J.V. Kilmartin. 1990. Components of the yeast spindle and spindle pole body. *J. Cell Biol.* 111:1913–1927.

Salmon, E.D., and R.R. Segall. 1980. Calcium-labile mitotic spindles isolated from sea urchin eggs (*Lytechinus variegatus*). *J. Cell Biol.* 86:355–365.

Salmon, E.D., D. Goode, T.K. Maugel, and D.B. Bonar. 1976. Pressure-induced depolymerization of spindle microtubules. III. Differential stability in HeLa cells. *J. Cell Biol.* 69:443–454.

Salmon, E.D., M. McKeel, and T. Hays. 1984. Rapid rate of tubulin dissociation from microtubules in the mitotic spindle in vivo measured by blocking polymerization with colchicine. *J. Cell Biol.* 99:1066–1075.

Saunders, W.S., and M.A. Hoyt. 1992. Kinesin-related proteins required for structural integrity of the mitotic spindle. *Cell.* 70:451–458.

Saunders, W., D. Hornack, V. Lengyel, and C. Deng. 1997a. The *Saccharomyces cerevisiae* kinesin-related motor Kar3p acts at preanaphase spindle poles to limit the number and length of cytoplasmic microtubules. *J. Cell Biol.* 137: 417–431.

Saunders, W., V. Lengyel, and M.A. Hoyt. 1997b. Mitotic spindle function in *Saccharomyces cerevisiae* requires a balance between different types of kinesin-related motors. *Mol. Biol. Cell.* 8:1025–1033.

Sherman, F., G.R. Fink, and J.B. Hicks. 1983. Methods in Yeast Genetics. Cold Spring Harbor Press, Cold Spring Harbor, NY.

Sikorski, R.S., and P. Hieter. 1989. A system of shuttle vectors and yeast host strains designed for efficient manipulation of DNA in *Saccharomyces cerevisiae*. *Genetics.* 122:19–27.

Winey, M., C.L. Mamay, E.T. O'Toole, D.N. Mastronarde, T.H. Giddings, Jr., K.L. McDonald, and J.R. McIntosh. 1995. Three-dimensional ultrastructural analysis of the *Saccharomyces cerevisiae* mitotic spindle. *J. Cell Biol.* 129: 1601–1616.

Yen, T.J., D.A. Compton, D. Wise, R.P. Zinkowski, B.R. Brinkley, W.C. Earnshaw, and D.W. Cleveland. 1991. CENP-E, a novel human centromere-associated protein required for progression from metaphase to anaphase. *EMBO (Eur. Mol. Biol. Organ.) J.* 10:1245–1254.

Zhai, Y., P.J. Kronebusch, and G.G. Borisy. 1995. Kinetochore microtubule dynamics and the metaphase-anaphase transition. *J. Cell Biol.* 131:721–734.

Zhang, D., and R.B. Nicklas. 1995. The impact of chromosomes and centrosomes on spindle assembly as observed in living cells. *J. Cell Biol.* 129: 1287–1300.